*Proc. Budapest'02 Workshop on*
*Quark & Hadron Dynamics* (2002) 000–000

**Budapest'02 Workshop on**
**Quark & Hadron Dynamics**
**Budapest, Hungary**
**March 3–7, 2002**

# Heavy Quark Production in Heavy Ion Colliders

R. Vogt

Physics Department, University of California, Davis, CA 95616
and
Nuclear Science Division, Lawrence Berkeley National Laboratory
University of California, Berkeley, California 94720, USA

**Abstract.** We describe updated calculations of $Q\overline{Q}$ production in $pp$ and $\pi^- p$ interactions. We compare these results to total cross section data and discuss how the baseline cross sections extrapolate to heavy ion collider energies. We touch upon the differences between leading and next-to-leading order heavy quark production. Finally, we discuss the implications of our calculations for quarkonium production. Our discussion here focuses on bottom quarks.

*Keywords:* heavy quarks, perturbative QCD
*PACS:* 25.75.-q

## 1. Introduction

Heavy quark production is of great relevance for high energy nuclear collisions. The large heavy quark masses means that their production can be calculated in perturbative QCD. They are produced in the initial nucleon-nucleon collisions and, as such, provide valuable information about the early state of the system. It is therefore important to make systematic studies to obtain the fullest possible information. The baseline rates in $pp$ interactions are essential to determine the expected total cross sections and the unmodified quark distributions.

There are many effects which can be studied through systematic heavy quark measurements. Heavy quark decays are expected to dominate the lepton pair continuum from the $J/\psi(c\overline{c})$ and $\Upsilon(b\overline{b})$ up to the mass of the $Z^0$ [1–3]. Thus the Drell-Yan yield and any thermal dilepton production will essentially be hidden by the heavy quark decay contributions [1]. The shape of the charm and bottom contributions to this continuum could be significantly altered by heavy quark energy loss [2, 4]. Since $B$ mesons decay to $J/\psi$, the secondary $J/\psi$ spectrum could be modified by energy loss effects on the primary $B$ [2]. If the heavy quark energy loss is large, it may be possible to extract a thermal dilepton yield if it cannot be determined by other means [5]. Heavy quark production in a quark-gluon plasma has also been predicted [6]. This additional yield can only be determined if the relative $AA/pp$ rate can be accurately measured. Finally, the $c\overline{c}$ yield is a useful reference for $J/\psi$ production since a $\langle J/\psi\rangle/\langle c\overline{c}\rangle$ enhancement has been predicted due to $c\overline{c}$ recombination [7–10]. This recombination requires more than one $c\overline{c}$ pair produced in an event, easily reached in heavy ion collisions at RHIC and LHC.

An update to the $pp$ baseline is relevant now because the gluon distributions have changed significantly since the calculations of Ref. [11]. The rise at low momentum fractions, $x$, is not as large as previously expected, significantly lowering the $c\overline{c}$ cross sections in particular. Less attention has been paid to the $b\overline{b}$ cross sections, perhaps due to a lack of $pp$ data. However, since a new measurement has recently become available [12], we will try to make up for this shortcoming here by concentrating on bottom production.

## 2. $Q\overline{Q}$ Total Cross Sections

At leading order (LO) heavy quarks are produced by $gg$ fusion and $q\overline{q}$ annihilation while at next-to-leading order (NLO) $qg$ and $\overline{q}g$ scattering is also included. To any order, the partonic cross section may be expressed in terms of dimensionless scaling functions $f_{ij}^{(k,l)}$ that depend only on the variable $\eta$ [13],

$$\hat{\sigma}_{ij}(\hat{s}, m_Q^2, \mu^2) = \frac{\alpha_s^2(\mu)}{m^2} \sum_{k=0}^{\infty} \, (4\pi\alpha_s(\mu))^k \sum_{l=0}^{k} \, f_{ij}^{(k,l)}(\eta) \, \ln^l \left(\frac{\mu^2}{m_Q^2}\right) \, , \tag{1}$$

where $\hat{s}$ is the partonic center of mass energy squared, $m_Q$ is the heavy quark mass, $\mu$ is the scale and $\eta = \hat{s}/4m_Q^2 - 1$. The cross section is calculated as an expansion in powers of $\alpha_s$ with $k = 0$ corresponding to the Born cross section at order $\mathcal{O}(\alpha_s^2)$. The first correction, $k = 1$, corresponds to the NLO cross section at $\mathcal{O}(\alpha_s^3)$. It is only at this order and above that the dependence on renormalization scale, $\mu_R$, enters the calculation since when $k = 1$ and $l = 1$, the logarithm $\ln(\mu^2/m_Q^2)$ appears. The dependence on the factorization scale, $\mu_F$, the argument of $\alpha_s$, appears already at LO. We assume that $\mu_R = \mu_F = \mu$. The next-to-next-to-leading order (NNLO) corrections to next-to-next-to-leading logarithm have been calculated near threshold [13] but the complete calculation only exists to NLO.

The total hadronic cross section is obtained by convoluting the total partonic cross section with the parton distribution functions (PDFs) of the initial hadrons,

$$\sigma_{pp}(s, m_Q^2) = \sum_{i,j=q,\overline{q},g} \int_{\frac{4m_Q^2}{s}}^{1} \frac{d\tau}{\tau} \, \delta(x_1 x_2 - \tau) \, F_i^p(x_1, \mu^2) F_j^p(x_2, \mu^2) \, \hat{\sigma}_{ij}(\tau, m_Q^2, \mu^2) \, , \tag{2}$$

where the sums $i$ and $j$ are over all massless partons and $x_1$ and $x_2$ are fractional momenta. The PDFs, denoted by $F_i^p$, are evaluated at scale $\mu$. All our calculations are fully NLO, applying NLO parton distribution functions and the two-loop evaluation of $\alpha_s$ to both the $\mathcal{O}(\alpha_s^2)$ and $\mathcal{O}(\alpha_s^3)$ contributions, as is typically done [13, 14].

To obtain the $pp$ cross sections at the RHIC and LHC proton and ion energies, we first compare the NLO cross sections to the available $c\bar{c}$ and $b\bar{b}$ production data by varying the mass, $m_Q$, and scale, $\mu$, to obtain the 'best' agreement with the data for several combinations of $m_Q$, $\mu$, and PDF. These 'best' fits aim to describe the available data without a scaling factor, the experimental '$K$' factor. We use the recent MRST HO central gluon [15], CTEQ 5M [16], and GRV 98 HO [17] distributions. The results for the $b\bar{b}$ cross section in $\pi^- p$ interactions, where there are the most data, are shown in Fig. 1 for the MRST HO densities with the SMRS pion densities [18]. We calculate the NLO cross sections for $4.25 \leq m_b \leq 5$ GeV with

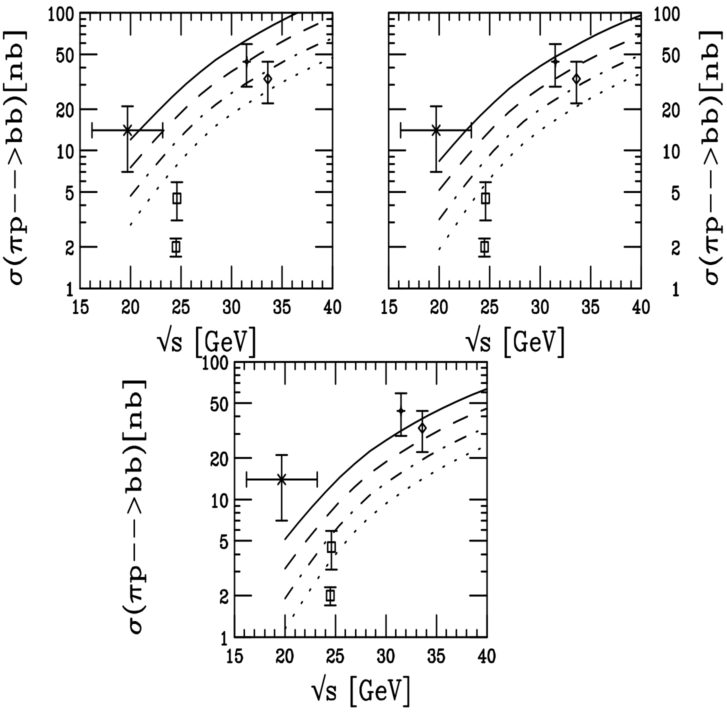


**Fig. 1.** Total $b\bar{b}$ cross sections in $\pi^- p$ interactions at fixed-target energies as a function of the bottom quark mass. All calculations are fully NLO using the MRST HO (central gluon) parton densities. From the upper left, the plots show results with the renormalization and factorization scales equal to $m_b/2$, $m_b$ and $2m_b$ respectively. In each plot, from top to bottom the curves are $m_b = 4.25$, 4.5, 4.75, and 5 GeV. The $b\bar{b}$ data can be found in Ref. [11].

scale choices clockwise from the upper left: $\mu = m_b/2$, $m_b$, and $2m_b$. The cross sections decrease as $\mu$ increases because $\alpha_s(m_b/2) > \alpha_s(m_b) > \alpha_s(2m_b)$ by the running of $\alpha_s$. Evolution of the PDFs with $\mu$ tends to go in the opposite direction *e.g.* the sea quark and gluon distributions rise as $x$ decreases while $\mu$ increases. At higher scales the two effects tend to compensate and reduce the scale dependence but the charm quark mass is not large enough for this to occur. The results for bottom quarks are somewhat better since the mass is larger.

We find reasonable agreement with all three PDFs for $m_b = \mu = 4.75$ GeV, $m_b = \mu/2 = 4.5$ GeV (dashed), and $m_b = 2\mu = 5$ GeV, shown in the right hand side of Fig. 2. The MRST results cluster together and lie a bit higher than the GRV 98 results for $\pi^- p$ production while the opposite is true for $pp$ production. The three data points from $pp \to b\overline{b}$ measurements lie somewhat closer together although the E789 point (the square on the left hand side of Fig. 2) lies considerably below the other two points. In fact, it agrees best with the NLO calculations using a 'standard' $b$ quark mass of 4.75 GeV.

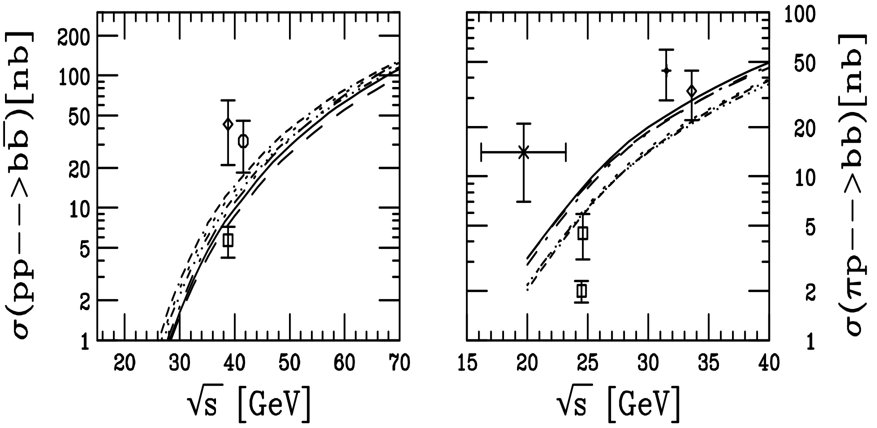


**Fig. 2.** Total $b\overline{b}$ cross sections in $pp$ and $\pi^- p$ interactions compared to data. All calculations are fully NLO. The curves are: MRST HO (central gluon) with $m_b = \mu = 4.75$ GeV (solid), $m_b = \mu/2 = 4.5$ GeV (dashed), and $m_b = 2\mu = 5$ GeV (dot-dashed); as well as the GRV 98 HO distributions with $m_b = \mu = 4.75$ GeV (dotted), $m_b = \mu/2 = 4.5$ GeV (dot-dot-dot-dashed), and $m_b = 2\mu = 5$ GeV (dot-dash-dash-dashed). The $pp$ data are from the E789 (square) [19], E771 (diamond) [20] and preliminary HERA-B (circle) [12] collaborations.

The somewhat larger spread in the $\pi^- p$ calculations may be because the $\pi^-$ PDFs are not very well known. The last evaluations, SMRS [18], Owens-$\pi$ [21], and GRV-$\pi$ [22] were 10-15 years ago and do not reflect any of the latest information on the low $x$ behavior of the proton PDFs, *e.g.* the distributions are all flat as $x \to 0$ with no low $x$ rise. The GRV distributions are based on dynamical parton densities with low initial scale which generate larger densities at low $x$ while depleting them at high $x$, reducing the $b\overline{b}$ cross sections at low $\sqrt{s}$ relative to the flat distributions of SMRS, see Fig. 2. These pion evaluations also depend on the behavior of the proton PDFs used in the original fit, including the value of $\Lambda_{\rm QCD}$. Thus the pion and proton PDFs are generally incompatible. The typical $x$ values of $b\overline{b}$ production are large, $0.14 \leq x = 2\mu/\sqrt{s} \leq 0.9$. At the fixed target energies of $b\overline{b}$ production, $q\overline{q}$ annihilation dominates while $gg$ fusion is still most important for $c\overline{c}$ production [23]. The valence-valence $\overline{u}_\pi u_p$ contribution dominates since the valence distributions are greatest at large $x$.

For charm production, the 'best' agreement with $\mu = m_c$ is for $m_c = 1.4$ GeV and $m_c = 1.2$ GeV is the best choice for $\mu = 2m_c$ for the MRST HO and CTEQ 5M distributions. The best agreement with GRV 98 HO is $\mu = m_c = 1.3$ GeV while the results with $\mu = 2m_c$ lies below the data for all $m_c$. All five results agree very well with each other for $pp \rightarrow c\overline{c}$. There is also more of a spread in the $\pi^- p \rightarrow c\overline{c}$ results. The $\pi^- p \rightarrow c\overline{c}$ cross sections are a bit lower than the data compared to the $pp$ cross sections, suggesting that lighter quark masses would tend to be favored. The reason is because the low $x$ rise in the proton PDFs depletes the gluon density for $x > 0.02$ relative to a constant at $x \rightarrow 0$ for $\mu = \mu_0$ the initial scale of the PDF. The $\pi^- p$ data are also in a relatively large $x$ region, $0.1 \leq x = 2\mu/\sqrt{s} \leq 0.3$, where this difference is important. For the $c\overline{c}$ results, see Ref. [24].

Before calculating the $Q\overline{Q}$ cross sections at nuclear colliders, some comments need to be made about the validity of the procedure. Since the $c\overline{c}$ calculations can only be made to agree with the data when somewhat lower than average quark masses are used and even the $pp \rightarrow b\overline{b}$ data suggest $m_b$ should be smaller, it is reasonable to expect that higher order corrections beyond NLO could be large. Indeed, the preliminary HERA-B cross section agrees with the NNLO-NNLL cross section in Ref. [13], suggesting that the next order correction could be nearly a factor of two. Thus the NNLO correction could be nearly as large as the NLO cross section.

Unfortunately, the NNLO-NNLL calculation is not a full result and is valid only near threshold. The $p\overline{p}$ data at higher energies, while not total cross sections, also show a large discrepancy between the perturbative NLO result and the data, nearly a factor of three [25]. This difference could be accounted for using unintegrated parton densities [26] although these unintegrated distributions vary widely at this point. The problem is then how to connect the regimes where near-threshold corrections are applicable and where high-energy, small $x$ physics dominates. The problem is increased for charm where, even at low energies, we are far away from threshold.

Our method is perhaps the easiest thing to try–using NLO only and ignoring higher-order corrections to fit the data. This is not difficult for $c\overline{c}$ because the data are extensive. However, there is less $b\overline{b}$ data to go on. The $\pi^- p \rightarrow c\overline{c}$ data tends to favor lighter masses. It is difficult to say if the same is true for $b\overline{b}$. A value of $m_b = 4.75$ GeV, which underpredicts the Tevatron results compared to NLO cross sections [25], agrees reasonably with the average of the $\pi^- p$ data. However, for the HERA-B measurement to be compatible with a NLO evaluation, the $b$ quark mass would have to be reduced to 4.25 GeV, a value which might be more compatible with the Tevatron results. Therefore, if the NNLO cross section could be calculated fully, the results would likely be more compatible with a larger quark mass. A quantitative statement is not possible at this time.

If we then assume that the NNLO and higher orders to not have a substantially different energy dependence than the LO and NLO results, then we will be in the right ballpark at collider energies. If the LO and NLO matrix elements are both evaluated with NLO PDFs and the two-loop $\alpha_s$, the theoretical $K$ factors have a relatively weak $\sqrt{s}$ dependence, $\leq 50\%$ for $20\,\mathrm{GeV} \leq \sqrt{s} \leq 14\,\mathrm{TeV}$. The produced heavy quark distributions might be slightly affected since the shapes are somewhat sensitive to the quark mass but charm is far enough above threshold at ion colliders for the effect to be small. A somewhat larger effect might be expected for bottom.

We now extrapolate our results to RHIC and LHC energies. The $b\bar{b}$ cross section is shown in Fig. 3. The spread in the $b\bar{b}$ cross sections is small, $\sim 20-30\%$ at the

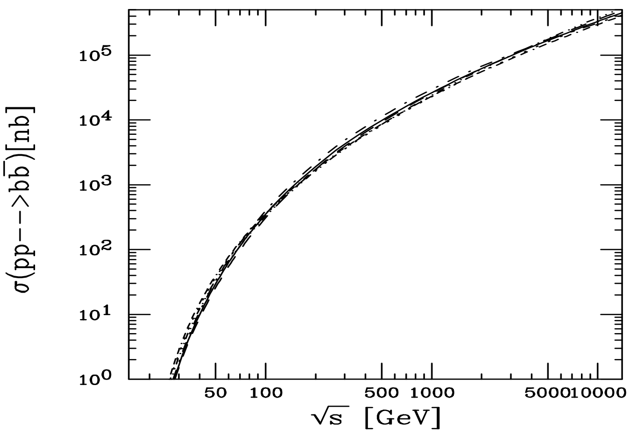


**Fig. 3.** Total $b\bar{b}$ cross sections in $pp$ interactions up to 14 TeV. All calculations are fully NLO. The curves are the same as in Fig. 2.

ion collider energies. The $c\bar{c}$ cross sections, on the other hand, differ by a factor of two at 5.5 TeV.

Defining the theoretical $K$ factor as NLO/LO, where both the numerator and denominator are calculated with NLO PDFs and the two-loop $\alpha_s$, is not the only way to proceed. It is, however, the most common because, in general, one wants to determine the size of the corrections. In principle, it is most correct to use LO PDFs and the one-loop $\alpha_s$ with the LO matrix elements and NLO PDFs and the two-loop $\alpha_s$ only with the $\mathcal{O}(\alpha_s^3)$ corrections. Since the QCD scale, $\Lambda$, is tuned to fit all available data in global analyses of parton distributions, whether at LO or NLO, the number of loops in the evaluation of $\alpha_s$ is important. When a fully LO calculation of the charm cross section is done with a one loop evaluation of $\alpha_s$ in the global analyses of the parton densities, as with the MRST LO set, the LO cross sections increase by $\sim 60\%$. This change is almost solely due to the difference between the one and two loop evaluations of $\alpha_s$. The MRST LO $\Lambda$ is 0.204 GeV when $n_f = 3$, leading to $\alpha_s^{1-\rm loop} = 0.287$ and $\alpha_s^{2-\rm loops} = 0.220$ for $\mu = 2m_c$. The $\Lambda$ associated with the MRST HO set is larger, $\Lambda = 0.353$ GeV when $n_f = 3$, corresponding to $\alpha_s^{1-\rm loop} = 0.364$ and $\alpha_s^{2-\rm loops} = 0.263$ at the same scale. The shapes of the LO and NLO PDFs are also somewhat different which can affect results in different regions.

A third way of defining the theoretical $K$ factor is also possible. One could compare a fully NLO calculation, where the LO and NLO matrix elements are calculated with $\alpha_s$ at two loops and a NLO PDF, with a LO calculation where the LO matrix elements are calculated with $\alpha_s$ at one loop and a LO PDF. This procedure is possibly most favored *e.g.* in event generators where most processes are calculated with LO matrix elements only. The magnitude of the theoretical $K$ factor depends on the chosen definition. Work is in progress to compare all three ways of evaluating the $K$ factor for heavy quark production [27].

Note that while the total cross section predicts the yield of heavy quark production over all phase space, it cannot provide much useful information on nuclear effects such a $p_T$-broadening and shadowing. Any broadening will not affect the total cross section but will have a strong influence on the $p_T$ distributions. Shadowing may reduce or enhance the nuclear cross section relative to that of the proton but the effect may be more apparent in some regions of phase space than others. To obtain more information on nuclear effects, it is thus necessary to turn to distributions. In addition, a real detector does not cover all phase space. The differential distributions can be tuned to a detector acceptance. For full details on the shadowing and broadening effects on the single quark and $Q\overline{Q}$ pair distributions, see Ref. [28]. It turns out that the $p_T$ distributions are more strongly influenced by any broadening effect than nuclear shadowing. Likewise, nuclear shadowing can best be studied combining information on rapidity and pair invariant mass distributions. The effect of shadowing on the dilepton continuum has been extensively studied in Ref. [29].

## 3. Relevance for Quarkonium

To better understand quarkonium in nuclear collisions, it is necessary to have a good estimate of the expected $pp$ yields. However, there are still a number of uncertainties in quarkonium production in $pp$ interactions. Two approaches have been used to describe quarkonium production phenomenologically—the color evaporation model (CEM) [30] and nonrelativistic QCD (NRQCD) [31].

In the CEM, the $Q\overline{Q}$ pair neutralizes its color by interaction with the collision-induced color field—“color evaporation”. The $Q$ and the $\overline{Q}$ either combine with light quarks to produce heavy-flavored hadrons or bind with each other in a quarkonium state. The additional energy needed to produce heavy-flavored hadrons is obtained nonperturbatively from the color field in the interaction region. The yield of all quarkonium states may be only a small fraction of the total $Q\overline{Q}$ cross section below the heavy hadron threshold, $2m_H$. The $Q\overline{Q}$ cross sections we have obtained through our 'by-eye' fits of the mass and scale parameters have implications for quarkonium if the CEM is used to calculate the production. This is because different quark masses will result in more or less of the cross section below the $2m_H$ threshold. Since we have concentrated on $b\overline{b}$ production in these proceedings, we show our results for $\Upsilon$ production where there is the biggest variation in mass and scale: $m_b = 4.5$ GeV is $0.85\,m_B$ while $m_b = 5$ GeV is $0.95\,m_B$, much closer to the $B\overline{B}$ threshold. Since the NRQCD cross section is obtained independently of the parameters used to calculate heavy quark production, we do not discuss it here.

At leading order, the production cross section of quarkonium state $C$ is

$$\sigma_C^{\rm CEM} = F_C \sum_{i,j} \int_{4m_Q^2}^{4m_H^2} d\hat{s} \int dx_1 dx_2 \; f_{i/p}(x_1) \; f_{j/p}(x_2) \; \hat{\sigma}_{ij}(\hat{s}) \; \delta(\hat{s} - x_1 x_2 s) \; , \tag{3}$$

where $ij = q\overline{q}$ or $gg$ and $\hat{\sigma}_{ij}(\hat{s})$ is the $ij \rightarrow Q\overline{Q}$ subprocess cross section. Hadronization is assumed not to affect the kinematics of the parent $Q\overline{Q}$ pair so that only a single universal factor, $F_C$, is necessary for the cross section of each state. The factor $F_C$ depends on the heavy quark mass, $m_Q$, the scale $\mu$ in the strong coupling constant $\alpha_s$ and the parton densities. The factor $F_C$ must be constant for the model to have any predictive power. The CEM was taken to NLO using exclusive $Q\overline{Q}$ hadroproduction [14] to obtain the energy, $x_F$, and $p_T$-dependence of quarkonium production [32,33]. In the CEM, $gg \rightarrow g(g^* \rightarrow Q\overline{Q})$, incorporated at NLO, is similar to models of $g^* \rightarrow \Upsilon$ fragmentation [34]. By including this splitting, the CEM provides a good description of the quarkonium $p_T$ distributions at the Tevatron. The CEM cross sections were calculated with the MRST HO [15] parton densities using the same values as the NLO evaluations of the heavy quark cross sections shown here. The values of $F_C$ for charmonium and bottomonium have been calculated from a fit to the $J/\psi$ and $\Upsilon$ data combined with relative cross sections and branching ratios, see Refs. [35,36] for details. The combined $\Upsilon$, $\Upsilon'$ and $\Upsilon''$ cross sections to muon pairs are compared to our CEM calculations in Fig. 4. We find that the direct $\Upsilon(1S)$ production cross section is $\approx 3.4$ nb at $\sqrt{s} = 200$ GeV and varies between 126-259 nb at 5.5 TeV.

## Acknowledgements

I would like to thank the HERA-B collaboration for keeping me informed about their exciting new data. This work was supported by the Director, Office of Energy Research, Office of High Energy and Nuclear Physics, Nuclear Physics Division of the U.S. Department of Energy under Contract No. DE-AC03-76SF00098.

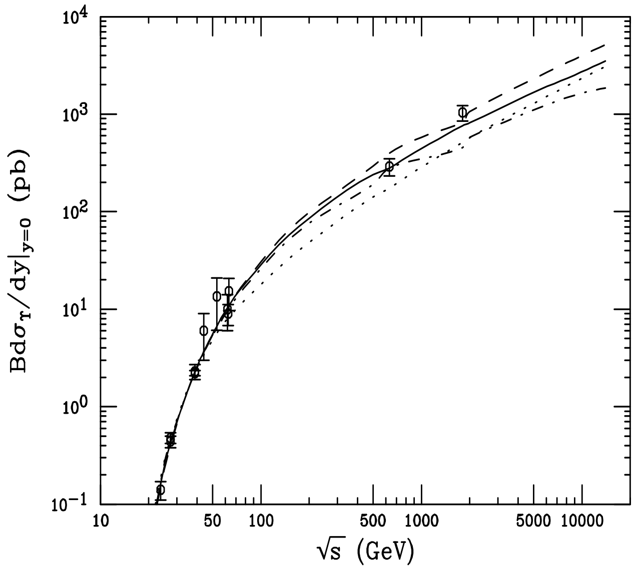


**Fig. 4.** Inclusive $\Upsilon$ production data, combined from all three $S$ states, and compared to NLO CEM calculations. The solid curve employs the MRST HO distributions with $m_b = \mu = 4.75$ GeV, the dashed, $m_b = \mu/2 = 4.5$ GeV, the dot-dashed, $m_b = 2\mu = 5$ GeV, and the dotted, GRV 98 HO with $m_b = \mu = 4.75$ GeV.

## References

1. S. Gavin, P.L. McGaughey, P.V. Ruuskanen and R. Vogt, *Phys. Rev.* **C54** 2606, (1996).
2. I.P. Lokhtin and A.M. Snigirev, *Eur. Phys. J.* **C21** (2001) 155.
3. G. Baur *et al.*, CMS NOTE 2000/060.
4. Z. Lin and R. Vogt, *Nucl. Phys.* **B544** (1999) 339.
5. K. Gallmeister, B. Kämpfer and O.P. Pavlenko, *Eur. Phys. J.* **C8** (1999) 473.
6. A. Shor, *Phys. Lett.* **B215** (1988) 375; *Phys. Lett.* **B233** (1989) 231; B. Müller and X.-N. Wang, *Phys. Rev. Lett.* **68** (1992) 2437; P. Lévai and R. Vogt, *Phys. Rev.* **C56** (1997) 2707.
7. P. Braun-Munzinger and J. Stachel, *Phys. Lett.* **B490** (2000) 196; *Nucl. Phys.* **A690** (2001) 119.
8. M.I. Gorenstein, A.P. Kostyuk, H. Stöcker and W. Greiner, *Phys. Lett.* **B509** (2001) 277; *J. Phys.* **G27** (2001) L47; M.I. Gorenstein, A.P. Kostyuk, H. Stöcker and W. Greiner, hep-ph/0012292.
9. L. Grandchamp and R. Rapp, *Phys. Lett.* **B523** (2001) 60.
10. R.L. Thews, M. Schroedter and J. Rafelski, *Phys. Rev.* **C63** (2001) 054905;

R.L. Thews, in proceedings of 'Statistical QCD', Bielefeld, Aug. 2001, edited by F. Karsch *et al.*, hep-ph/0111015.
11. P.L. McGaughey *et. al.*, *Int. J. Mod. Phys.* **A10** (1995) 2999.
12. M. Villa (HERA-B Collab.), private communication.
13. N. Kidonakis, E. Laenen, S. Moch, and R. Vogt, *Phys. Rev.* **D64** (2001) 114001.
14. M.L. Mangano, P. Nason and G. Ridolfi, *Nucl. Phys.* **B405** (1993) 507.
15. A.D. Martin, R.G. Roberts, W.J. Stirling and R.S. Thorne, *Eur. Phys. J.* **C4** (1998) 463; *Phys. Lett.* **B443** (1998) 301.
16. H.L. Lai *et al.*, *Eur. Phys. J.* **C12** (2000) 375.
17. M. Glück, E. Reya and A. Vogt, *Eur. Phys. J.* **C5** (1998) 461.
18. P.J. Sutton, A.D. Martin, R.G. Roberts and W.J. Stirling, *Phys. Rev.* **D45** (1992) 2349.
19. D.M. Jansen *et al.* (E789 Collab.), *Phys. Rev. Lett.* **74** (1995) 3118.
20. T. Alexopoulos *et al.* (E771 Collab.), *Phys. Rev. Lett.* **82** (1999) 44.
21. J.F. Owens, *Phys. Rev.* **D30** (1984) 943.
22. M. Glück, E. Reya and A. Vogt, *Z. Phys.* **C53** (1992) 651.
23. J. Smith and R. Vogt, *Z. Phys.* **C75** (1997) 271.
24. R. Vogt, in proceedings of the '18$^{\rm th}$ Winter Workshop on Nuclear Dynamics', Nassau, The Bahamas, edited by W. Bauer *et al.*, hep-ph/0203152.
25. T. Affolder *et al.* (CDF Collab.), *Phys. Rev. Lett.* **84** (2002) 232.
26. A.P. Lipatov, V.A. Saleev and N.P. Zotov, hep-ph/0112114.
27. R. Vogt, in preparation.
28. R. Vogt, to appear in the Proceedings of the Hard Probe Collaboration, LBNL-45350, hep-ph/0111271.
29. K.J. Eskola, V. Kolhinen and R. Vogt, *Nucl. Phys.* **A696** (2001) 729.
30. V. Barger, W.Y. Keung, and R.N. Philips, *Z. Phys.* **C6** (1980) 169; *Phys. Lett.* **91B** (1980) 253.
31. G.T. Bodwin, E. Braaten, and G.P. Lepage, *Phys. Rev.* **D51** (1995) 1125.
32. R.V. Gavai *et al.*, *Int. J. Mod. Phys.* **A10** (1995) 3043.
33. G.A. Schuler and R. Vogt, *Phys. Lett.* **B387** (1996) 181.
34. E. Braaten, M.A. Doncheski, S. Fleming and M.L. Mangano, *Phys. Lett.* **B333** (1994) 548.
35. J.F. Gunion and R. Vogt, *Nucl. Phys.* **B492** (1997) 301.
36. S. Digal, P. Petreczky, and H. Satz, *Phys. Rev.* **D64** (2001) 094015.